

BCS-BEC Crossover and Topological Phase Transition in Spin-Orbit Coupled Degenerate Fermi Gases

Ming Gong¹, Sumanta Tewari², and Chuanwei Zhang^{1*}

¹*Department of Physics and Astronomy, Washington State University, Pullman, WA, 99164 USA*

²*Department of Physics and Astronomy, Clemson University, Clemson, SC 29634 USA*

Ultra-cold degenerate Fermi gases (DFG) with population imbalance (equivalent to an effective Zeeman field) have sparked tremendous recent interest in both theory and experiment. The recent experimental realization of spin-orbit coupling (SOC) opens another new avenue for the study of DFG. In this Letter, we investigate the BCS-BEC crossover physics in DFG with both Zeeman field and SOC. We show that the superfluid order parameter destroyed by a large Zeeman field can be restored by SOC. At zero temperature, there is a topological phase transition in such systems from a non-topological superfluid to a topological superfluid with increasing Zeeman fields or by tuning the s -wave scattering length. The two phases are separated by a critical point which itself is a gapless superfluid. We show how the zero-temperature topological quantum phase transition can be probed at finite temperatures using cold atom photoemission spectroscopy which has already been realized in experiments.

PACS numbers: 03.75Ss, 74.20.-z, 03.75.Lm

Introduction: Ultra-cold DFG with tunable atom interaction through Feshbach resonance [1] have garnered tremendous attention recently [2] for their potential use as an ideal platform for emulating many important physical phenomena, ranging from high temperature superconductivity to quark-gluon plasma and neutron stars [3]. Interesting physics, including the crossover from BCS superfluid to BEC of molecules [4–6], universal properties in the unitary limit [7], vortices [8], *etc.*, have been observed in experiments. In addition to single species Fermi atoms with equal population in two spin states, DFG with population and mass imbalance have also been intensively studied [9–11]. Here the population imbalance between two pseudo-spin states serves as an effective Zeeman field, which have stimulated enormous experimental efforts on searching for the FFLO state in DFG [12].

The pseudospin of atoms can couple with not only the effective Zeeman field, but also with the orbital degrees of freedom of atoms (*i.e.*, SOC). SOC for electrons has played a crucial role in condensed matter physics and has led to many important phenomena, such as spin and anomalous Hall effects [13], topological insulator [14], *etc.* On the other hand, the recent experimental realization of SOC for ultra-cold atoms [15] opens a completely new avenue for investigating the physics in DFG. In this context, it should be not only natural but also interesting to investigate the BCS-BEC crossover physics [16, 17] in the presence of SOC. The crossover physics is also important because the s -wave superfluid, together with SOC and Zeeman field, may yield intriguing chiral p -wave physics [18] with non-trivial statistical properties. For example, Majorana fermions and the associated non-Abelian statistics, the critical ingredients for performing topological quantum computation [19], may be observable only in the crossover region where the superfluid order parameter is large and thus robust against finite

temperature effects.

In this Letter, we investigate the BCS-BEC crossover in a uniform s -wave superfluid in the presence of both Zeeman field and Rashba-type of SOC. Without SOC, it is well known that the superfluid order parameter vanishes beyond a critical Zeeman field for a given s -wave interaction strength [20]. We show that a finite SOC strength can restore the superfluid order parameter back to the system even when the Zeeman field is well above the critical value. Our calculation is based on the mean field theory [2], where the superfluid order parameter and the chemical potential are obtained by solving the gap and the total atom number equations self-consistently. The Majorana fermions exist inside vortices or edges when the bulk superfluid is in the topological state [19]. We show that there is a series of finite-temperature phase crossovers, manifested by the change of the quasiparticle excitation spectrum, from a non-topological superfluid (NTS) to a gapless superfluid (GS) and then to a topological superfluid (TS) state with increasing values of the Zeeman field or by tuning the s -wave interaction strengths (At zero temperature the crossover lines meet at a quantum critical point separating the NTS and the TS states, see Fig. 4.). During this sequence, the quasiparticle excitation gap first closes and then reopens. This phenomenon can be detected using momentum resolved photoemission spectroscopy for cold atoms which has already been experimentally realized [21, 22]. The experimental detection of the crossover sequence can serve as a clear signature of the realization of the topological superfluid state in cold atom experiments.

Spin-orbit coupled DFG: The system we consider is a three-dimensional (3D) uniform s -wave fermionic superfluid with the atom density n and which is subject to Rashba SOC in the xy plane and a Zeeman field along the z direction. The dynamics of the Fermi gas can be

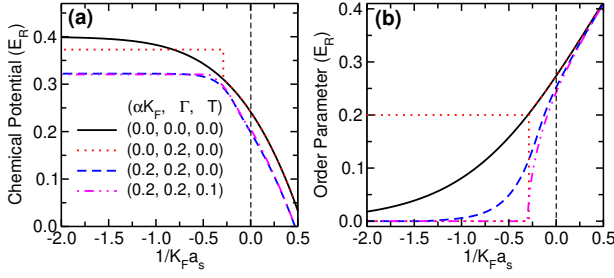


FIG. 1. (Color online) Plot of the chemical potential μ (a) and the order parameters Δ (b) versus $\nu = 1/K_F a_s$ for different parameters $(\alpha K_F, \Gamma, T)$.

described by the Hamiltonian,

$$H = H_0 + H_z + H_{\text{int}}, \quad (1)$$

where $H_0 = \sum_{\mathbf{k}\gamma\gamma'} c_{\mathbf{k}\gamma}^\dagger [\xi_{\mathbf{k}} I + \alpha (k_y \tau_x - k_x \tau_y)]_{\gamma\gamma'} c_{\mathbf{k}\gamma'}$, $\gamma = \uparrow, \downarrow$ are the pseudo-spin of the atoms, $\xi_{\mathbf{k}} = \epsilon_{\mathbf{k}} - \mu$, $\epsilon_{\mathbf{k}} = \hbar^2 k^2 / 2m$, μ is the chemical potential, α is the Rashba SOC strength which can be generated using atom-laser interaction [15, 23–25], τ_i is the Pauli matrix, and $c_{\mathbf{k}\gamma}$ is the atom annihilation operator. In solid state systems, SOC arises from certain inversion symmetry breaking and is usually very small (*i.e.*, $\alpha \ll \hbar^2 K_F / 2m$ with K_F as the Fermi vector); however, in ultracold atomic systems the region $\alpha \sim \hbar^2 K_F / 2m$ is attainable [23–25]. $H_z = \Gamma \sum_{\mathbf{k}} (c_{\mathbf{k}\uparrow}^\dagger c_{\mathbf{k}\uparrow} - c_{\mathbf{k}\downarrow}^\dagger c_{\mathbf{k}\downarrow})$ is the Zeeman piece of the Hamiltonian. $H_{\text{int}} = g \sum_{\mathbf{k}\mathbf{q}} c_{\mathbf{k}+\mathbf{q}\uparrow}^\dagger c_{-\mathbf{k}-\mathbf{q}\downarrow}^\dagger c_{-\mathbf{k}\downarrow} c_{\mathbf{k}\uparrow}$ is the s -wave scattering interaction with $g = 4\pi\hbar^2 \bar{a}_s / m$, and the s -wave scattering length \bar{a}_s can be tuned using the Feshbach resonance [1].

Because of the Rashba SOC, each single particle energy band contains both spin \uparrow and \downarrow components. Therefore it is convenient to work in the dressed state basis provided by the eigenstates $\phi_\lambda = (1 \ -i\lambda e^{i\theta_{\mathbf{k}}})^T / \sqrt{2}$ of H_0 , where $\lambda = \pm$ represent two dressed states with the eigenenergies $\omega_\lambda = \xi_{\mathbf{k}} + \lambda \alpha k$. The corresponding atom annihilation operator for the dressed state is $a_{\mathbf{k}\lambda} = (c_{\mathbf{k}\uparrow} + i\lambda e^{-i\theta_{\mathbf{k}}} c_{\mathbf{k}\downarrow}) / \sqrt{2}$. Without SOC, the Zeeman field lifts the spin degeneracy between \uparrow and \downarrow , thus destroys the Cooper pairing when the Zeeman field is larger than the pairing interaction energy [20]. With SOC, the lowest spin-orbit energy band contains both spin \uparrow and \downarrow components even with a large Zeeman field, leading to the superfluid Cooper pairing between two fermions in the same branch (+ or -) with opposite momenta.

The s -wave scattering interaction between atoms can be treated in the mean field approximation using the finite temperature Green function method [26], where the atom number and mean-field pairing gap of the superfluid are described by the normal and anomalous Green functions, $\mathcal{G}_{\lambda\lambda'}(\mathbf{k}, t - t') = -\langle T_t a_{\mathbf{k}\lambda}(t) a_{\mathbf{k}\lambda'}^\dagger(t') \rangle$, and $\mathcal{F}_{\lambda\lambda'}(\mathbf{k}, t - t') = \lambda \langle T_t a_{\mathbf{k}\lambda}(t) a_{-\mathbf{k}\lambda'}(t') \rangle$ in the dressed state basis. Here T_t is the time ordering parameter

and the operators $a_{\mathbf{k}\lambda}(t)$ are in the Heisenberg picture. Using the time evolution of the operator $a_{\mathbf{k}\lambda}(t)$ operator, $\partial_t a_{\mathbf{k}\lambda}(t) = [H, a_{\mathbf{k}\lambda}(t)]$, and introducing the superfluid gap equation $\Delta_{\lambda\lambda'}(\mathbf{k}) = \frac{g\lambda'}{4} \sum_{\mathbf{q}, \mu, \mu'} (1 + \lambda' \mu' e^{i\theta_{-\mathbf{k}} - i\theta_{-\mathbf{q}}}) (1 + \mu' \mu e^{i\theta_{\mathbf{k}} - i\theta_{\mathbf{q}}}) \mathcal{F}_{\lambda\lambda'}(\mathbf{k}, 0)$, we obtain the equation of motion [26, 27]

$$\mathcal{L}_\lambda (\bar{\mathcal{G}}_{\lambda\lambda}, \bar{\mathcal{G}}_{\bar{\lambda}\bar{\lambda}}, \bar{\mathcal{F}}_{\lambda\lambda}, \bar{\mathcal{F}}_{\bar{\lambda}\bar{\lambda}})^T = (1, 0, 0, 0)^T, \quad (2)$$

where $\bar{\mathcal{G}}_{\lambda\lambda'} = \mathcal{G}_{\lambda\lambda'}(\mathbf{k}, i\omega_n)$, $\bar{\mathcal{F}}_{\lambda\lambda'} = \mathcal{F}_{\lambda\lambda'}(\mathbf{k}, i\omega_n)$, $\mathcal{G}_{\lambda\lambda'}(\mathbf{k}, t) = \beta^{-1} \sum_n e^{-i\omega_n t} \mathcal{G}_{\lambda\lambda'}(\mathbf{k}, i\omega_n)$, $\beta = k_B T$, $\omega_n = (2n + 1)\pi/\beta$ is the Matsubara frequency, and

$$\mathcal{L}_\lambda = \begin{pmatrix} i\omega_n - \omega_\lambda & -\Gamma & \Delta_{\lambda\lambda} & \Delta_{\lambda\bar{\lambda}} \\ -\Gamma & i\omega_n - \omega_{\bar{\lambda}} & \Delta_{\bar{\lambda}\lambda} & \Delta_{\bar{\lambda}\bar{\lambda}} \\ \Delta_{\lambda\lambda}^* & \Delta_{\bar{\lambda}\lambda}^* & i\omega_n + \omega_\lambda & -\Gamma \\ \Delta_{\lambda\bar{\lambda}}^* & \Delta_{\bar{\lambda}\bar{\lambda}}^* & -\Gamma & i\omega_n + \omega_{\bar{\lambda}} \end{pmatrix}. \quad (3)$$

Because of the s -wave local contact interaction, it can be shown that $\Delta_{+-} = \Delta_{-+} = 0$ and $\Delta_{++} = \Delta_{--}^* \equiv \Delta$. The quasiparticle excitation spectrum is obtained by replacing $i\omega_n$ with ω in Eq. (3) and setting $\det \mathcal{L}_\lambda = 0$, leading to

$$E_\pm^2 = \xi_{\mathbf{k}}^2 + \alpha^2 \rho^2 + \Gamma^2 + |\Delta|^2 \pm 2E_0 \quad (4)$$

where $E_0 = \sqrt{\Gamma^2 (\xi_{\mathbf{k}}^2 + |\Delta|^2) + \alpha^2 \rho^2 \xi_{\mathbf{k}}^2}$ and $\rho = \sqrt{k_x^2 + k_y^2}$. For $\alpha = \Gamma = 0$, Eq. (4) reduces to $E_\pm^2 = \xi_{\mathbf{k}}^2 + |\Delta|^2$ in the standard BCS theory, where the quasiparticle excitation gap $E_g = \min_{\mathbf{k}} (E_-) = \Delta$ (here $\mu > 0$). From Eq. (4) we find, without SOC, $E_g = \min_{\mathbf{k}} \left| \sqrt{\xi_{\mathbf{k}}^2 + |\Delta|^2} - \Gamma \right| = 0$ when $|\Gamma| > \Delta$ by choosing a suitable \mathbf{k} , which destroys the Cooper pair and there is no superfluidity, as expected.

Eq. (2) yields the gap equation at finite temperatures,

$$\frac{m\Delta}{4\pi\hbar^2 a_s} = -\Delta \sum_{\mathbf{k}, \lambda} (1 - \lambda \Gamma^2 / E_0) f(E_\lambda) - \frac{1}{2\epsilon_{\mathbf{k}}}, \quad (5)$$

where $f(E_\lambda) = \tanh(\beta E_\lambda / 2) / 4E_\lambda$. In the above equation, the ultra-violet divergence has been regularized in a standard manner [2] and a_s is defined as the renormalized scattering length. The total particle number is given by $N = \sum_{\mathbf{k}, i\omega_n, \lambda} \mathcal{G}_{\lambda\lambda}(\mathbf{k}, i\omega_n)$. Using Eq. (2) we find,

$$N = 2 \sum_{\mathbf{k}, \lambda} [\lambda (\alpha^2 \rho^2 + \Gamma^2) / E_0 - 1] \xi_{\mathbf{k}} f(E_\lambda) + \frac{1}{2}. \quad (6)$$

BCS-BEC crossover: We self-consistently solve the gap equation (5) and the number equation (6) for different parameters $(\alpha K_F, \Gamma, \nu, T)$ for a fixed atom density n to determine Δ and μ . Here $\nu = 1/K_F a_s$ and $K_F = (3\pi^2 n)^{1/3}$ is the Fermi vector for a non-interacting Fermi gas with the same density at $\Gamma = \alpha = 0$. The energy unit is chosen as the atom recoil energy E_R . The fixed density n corresponds to a fixed Fermi energy

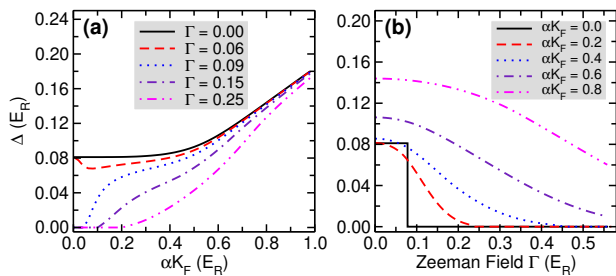


FIG. 2. (a) Plot of Δ with respect to αK_F for different Γ . (b) Plot of Δ with respect to Γ for different αK_F .

$E_F = \hbar^2 K_F^2 / 2m$. The momentum cutoff in the summation is chosen to be large enough to obtain converging results. Henceforth, we fix $E_F = 0.4E_R$ and have confirmed that similar results can be obtained for other E_F . In Fig. 1, we plot the change of μ and Δ with respect to ν for different $(\alpha K_F, \Gamma, T)$. In the BEC region, αK_F and Γ do not have significant influence on Δ because all fermion atoms form bound molecules. Hence we mainly focus on the BCS side. At $T = 0$ and $\alpha = 0$, the superfluid order parameter is destroyed when $\Gamma > \Delta$. In contrast, Δ and μ are independent of Γ when $\Gamma < \Delta$. This can be understood from the fact that, without SOC, Eq. (5) and (6) are independent of Γ when $\Gamma < \Delta$. Therefore there is a sudden jump of μ and Δ at $\Gamma = \Delta$ for $\alpha = 0$, as clearly seen from Fig. 1. The superfluid order parameter can be restored to non-zero values even for a large Γ when αK_F is switched on. As expected, the finite temperature can destroy the superfluid even with Rashba SOC.

In Fig. 2a, we plot Δ with respect to αK_F on the BCS side with $\nu = -1$ and $T = 0$. For other values of ν and T , the results are similar. When $\Gamma < \Delta$, the order parameter Δ approaches the same point for different Γ when $\alpha \rightarrow 0$. Δ vanishes for increasing Γ at $\alpha = 0$, but can be restored when α is nonzero. Therefore the superfluid order can still be observed even with a large Zeeman field. For example, when $\Gamma = 0.25$, significant order parameter can still be observed when $\alpha K_F = 0.4$. In Fig. 2b, we plot Δ versus Γ for different SOC. Without SOC, we observe a sudden jump of the order parameter at $\Gamma = \Delta$, as expected. With non-zero SOC, Δ decreases smoothly with Γ . At large Γ , the numerical results can be fitted with $\Delta \sim \eta \Gamma^{-2}$ with the constant η depending on SOC.

Topological phase transition: The quasiparticle excitation spectrum (4) shows very different properties in the presence of SOC. We find $E_{\mathbf{k},-} E_{\mathbf{k},+} = (\xi_{\mathbf{k}}^2 - \Gamma^2 + \Delta^2 - \alpha^2 \rho^2)^2 + 4\Delta^2 \alpha^2 \rho^2$, therefore there is always a finite gap along $\rho > 0$. In a 2D uniform superfluid (*i.e.*, $k_z = \text{constant}$),

$$E_g = |\Gamma - \sqrt{\bar{\mu}^2 + \Delta^2}| \quad (7)$$

is always finite when $\Gamma^2 \neq \Delta^2 + \bar{\mu}^2$ ($\bar{\mu} = \mu - \hbar^2 k_z^2 / 2m$).

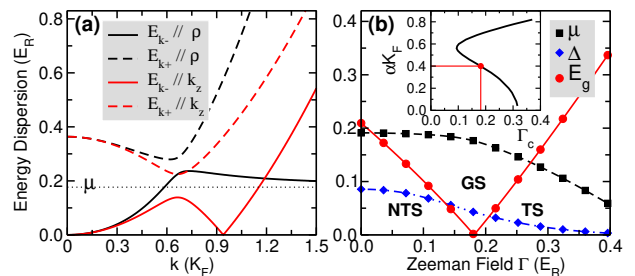


FIG. 3. (a) Plot of the quasiparticle energy dispersion along different momentum direction. (b) Plot of E_g , Δ , and μ , with respect to Γ at $\mathbf{k} = 0$. $\nu = -1.0$, $\alpha K_F = 0.4$, and $T = 0$. The dependence of the critical Γ_c on αK_F is shown in the inset.

In the region $\Gamma < \sqrt{\bar{\mu}^2 + \Delta^2}$, the system is a regular s -wave NTS. As Γ increases, E_g first vanishes (for $\rho = 0$) at the critical point $\Gamma_c = \sqrt{\bar{\mu}^2 + \Delta^2}$ and then reopens when $\Gamma > \sqrt{\bar{\mu}^2 + \Delta^2}$, where the superfluid becomes topologically non-trivial with Majorana zero energy excitations in the vortex core or the edge [28]. At Γ_c , the order parameter Δ is still continuous and finite (see Fig. 3b), although the quasiparticle excitation gap E_g has a node at certain ρ , therefore the system is a GS at Γ_c . We see there is a topological quantum phase transition from gapped NTS to GS (at the critical point) and then to gapped TS with increasing Zeeman fields. In a 3D system, the critical equation $\Gamma_c = \sqrt{\bar{\mu}^2 + \Delta^2}$ can always be satisfied for certain k_z and the superfluid becomes gapless at this k_z . However, for each fixed k_z in the excitation spectrum, the above topological phase transition always exists with increasing Γ . Note that although Eq. (7) is the same as that in the semiconductor heterostructure [28], the underlying physics is quite different. In the semiconductor heterostructure, μ and Δ can be induced externally and controlled independently. While in the cold atom system, they are constrained by the gap and particle number equations (5,6) and should be determined self-consistently. Therefore, the existence of TS in ultracold atom systems is not transparent.

In Fig. 3a, we plot E_{\pm} along the ρ (with $k_z = 0$) and the k_z (with $\rho = 0$) directions for $\Gamma_c = \sqrt{\bar{\mu}^2(\Gamma_c) + \Delta^2(\Gamma_c)}$. Clearly, the spectrum becomes gapless at $\rho = 0$ at the critical Γ_c . Along the k_z direction, there is another zero gap that does not disappear even for other Γ . In the presence of a strong confinement along the z direction (*i.e.*, the quasi-2D), only the lowest several energy bands along the z direction are occupied. Therefore the zero gap along the z direction is removed and the system is a gapped TS if Γ is larger than the critical Γ_c .

Next we show that the signature of the topological phase transition manifested in the quasiparticle energy spectrum can also be observed in a 3D uniform superfluid by considering only the part of the spectrum with a vanishing momentum along k_z (*i.e.*, $k_z = 0$). This is all

possible because the quasiparticle energy spectrum can be detected using the photoemission spectroscopy that is actually momentum resolved, as demonstrated in recent experiments [21, 22]. In Fig. 3b, we plot the quasiparticle excitation gap E_g at $\mathbf{k} = 0$ with respect to Γ at temperature $T = 0$. The corresponding Δ and μ are also plotted. When Γ sweeps through $\Gamma_c = 0.18$, E_g first closes and then reopens, indicating a transition $\text{NTS} \rightarrow \text{GS} \rightarrow \text{TS}$. At the critical point Γ_c , we still observe a strong superfluid order $\Delta_c = 0.043$. The critical Γ_c depends strongly on the SOC, as shown in the inset of Fig. 3b. There is a minimal value of Γ_c at $\alpha K_F \sim 0.59$, where $\mu \sim 0$ and $\sqrt{\mu^2 + \Delta^2}$ becomes minimal. This minimal value of Γ_c also depends on the scattering length, but is always larger than zero.

A realistic experiment only works at a finite temperature, which induces thermal fluctuation that may destroy the superfluid. The percentage of the thermal component in the gas depends strongly on the ratio between the quasiparticle excitation gap and the temperature. In Fig. 4a, we plot the phase boundary at which the ratio $\xi = 1.0$, this is,

$$E_g(\alpha, \nu, \Gamma, T) = \xi k_B T. \quad (8)$$

Note that E_g also depends on T , therefore Eq. (8) should be solved self-consistently in conjunction with Eq. (5) and (6) simultaneously. Note also that the relationship between Δ and Γ is quite different from the zero temperature case in Fig. 3b because the temperature is determined by Eq. (8) and not fixed now. As we increase Γ , the required order parameters first increase and then decrease to zero when $\Gamma > 0.256$ because at this point, the superfluid is destroyed by the finite temperature effect. In experiments, the fixed temperature corresponds to a horizontal line (with the arrow) in the phase diagram Fig. 4a. We see the phase crossover can be observed at finite temperature.

The topological phase transition can be observed by tuning not only the Zeeman field, but also the s -wave scattering length because Δ and μ have strong dependence on a_s . In Fig. 4b, we plot $\sqrt{\mu^2(\Gamma) + \Delta^2(\Gamma)} - \Gamma$ with respect to ν for fixed $\alpha K_F = 0.4$ and $T = 0.05$. The TS occur in the shadow region with nonzero Δ , $\sqrt{\mu^2(\Gamma) + \Delta^2(\Gamma)} - \Gamma < 0$, and $a_s < 0$ (BCS side). As $|\nu|$ increases in the BCS side, there is a transition from NTS to TS in certain parameter region, as clearly seen from Fig. 4b. The area for the TS depends strongly on the SOC and generally is bigger for larger SOC. Such topological phase transition driven by the s -wave scattering interaction cannot be observed in the solid state systems [28] where the pairing interaction cannot be varied.

Experimental observation: In experiments, the Rashba SOC and Zeeman field can be generated through the coupling between atoms and laser fields [15, 23–25]. For ^{40}K atom, $E_R = \hbar \times 8.7$ KHz, and $E_F = 0.4E_R = \hbar \times 3.5$ KHz, corresponding to the atom density $n = 5 \times 10^{12}$

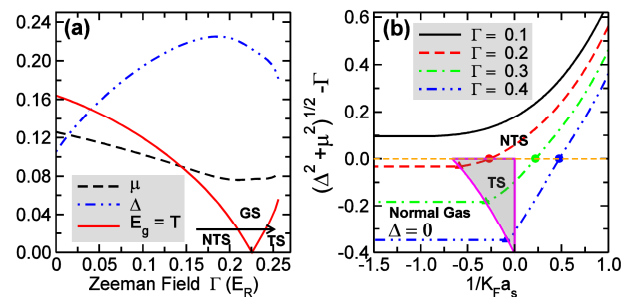


FIG. 4. (a) Plot of the topological phase crossovers (red curve) at finite temperatures, where the red curve is determined by Eq. 8. The arrow represents the phase crossovers at a fixed temperature. (b) Topological phase transition by varying the s -wave scattering length. The shadow region is the TS, with the three boundary lines determined by $(\Delta^2 + \mu^2)^{1/2} = \Gamma$, $1/k_F a_s = 0$, and $\Delta = 0$. $\alpha K_F = 0.4$ in both figures.

cm^{-3} . A large SOC strength $\alpha K_F \sim E_F$ is attainable. The s -wave scattering length can be tuned through the Feshbach resonance [1]. The existence of non-zero superfluid order parameters induced by the SOC with a large Zeeman field can be detected through the emergence of vortices [8] when an effective magnetic field is applied through direct rotation or the laser-atom interaction [29]. The topological phase transition can be observed by detecting the quasiparticle excitation gap E_g along certain momentum direction using the momentum resolved photoemission spectroscopy [21, 22]. In the experiment, the observed gap E_g first decreases to zero and then increases which is a clear signature of transition from NTS to TS.

Summary: In summary, stimulated by recent experimental progress in generating SOC in ultracold atoms, we study the BCS-BEC crossover physics and the topological phase transition in 3D uniform spin-orbit coupled DFG. The predicted SOC induced s -wave superfluid opens new possibilities for generating and observing many new topological phenomena in DFG. The observation of the topological phase transition from NTS to TS using the experimentally already realized photoemission spectroscopy provides a critical first step for searching for Majorana fermions and the associated non-Abelian statistics in cold atom s -wave superfluids, which are of not only fundamental but also technological importance.

Acknowledgement This work is supported by DARPA-YFA (N66001-10-1-4025), ARO (W911NF-09-1-0248), and DARPA-MTO (FA9550-10-1-0497).

* Corresponding author. Email: cwzhang@wsu.edu

[1] C. Chin *et al.*, Rev. Mod. Phys. **82**, 1225 (2010)
 [2] S. Giorgini *et al.*, Rev. Mod. Phys. **80**, 1215 (2008).
 [3] J. E. Thomas, Phys. Today **63**, 34 (2010).

- [4] C. A. Regal *et al.*, Phys. Rev. Lett. **92**, 040403 (2004).
- [5] M.W. Zwierlein *et al.*, Phys. Rev. Lett. **92**, 120403 (2004).
- [6] M. Bartenstein *et al.*, Phys. Rev. Lett. **92**, 120401 (2004)
- [7] J. T. Stewart *et al.*, Phys. Rev. Lett. **104**, 235301 (2010)
- [8] M. W. Zwierlein *et al.*, Nature **435**, 1047 (2005).
- [9] M. W. Zwierlein *et al.*, Science **311**, 492 (2006).
- [10] G. B. Partridge *et al.*, Science **311**, 503 (2006).
- [11] M. Taglieber *et al.*, Phys. Rev. Lett. **100**, 010401 (2008).
- [12] Y. Liao *et al.*, Nature **467**, 567 (2010).
- [13] D. Xiao *et al.*, Rev. Mod. Phys. **82**, 1959 (2010).
- [14] M. Z. Hasan, and C. L. Kane, Rev. Mod. Phys. **82**, 3045 (2010).
- [15] Y.-J. Lin *et al.*, Nature **471**, 83 (2011).
- [16] M. Holland *et al.*, Phys. Rev. Lett. **87**, 120406 (2001).
- [17] C. A. R. Sá de Melo, Phys. Today 61, 45 (2008).
- [18] C. Zhang *et al.*, Phys. Rev. Lett. **101**, 160401 (2008).
- [19] C. Nayak *et al.*, Rev. Mod. Phys. **80**, 1083 (2008).
- [20] P. F. Bedaque *et al.*, Phys. Rev. Lett. 91, 247002 (2003).
- [21] J. T. Stewart *et al.*, Nature **454**, 744 (2008).
- [22] J. P. Gaebler *et al.*, Nature Phys. **6**, 569 (2010).
- [23] J. Ruseckas *et al.*, Phys. Rev. Lett. **95**, 010404 (2005).
- [24] C. Zhang, Phys. Rev. A **82**, 021607(R) (2010).
- [25] D. L. Campbell *et al.*, arXiv:1102.3945.
- [26] G. D. Mahan, *Many-body Physics* (Plenum Press, New York 1981).
- [27] S. Tewari *et al.*, arXiv:1012.0057.
- [28] J. D. Sau *et al.*, Phys. Rev. Lett. **104**, 040502 (2010).
- [29] Y.-J. Lin *et al.*, Nature **462**, 628 (2009).